

Band geometry from position-momentum duality at topological band crossings

Yu-Ping Lin¹ and Wei-Han Hsiao²

¹*Department of Physics, University of Colorado, Boulder, Colorado 80309, USA*

²*Independent Researcher*

(Dated: May 23, 2022)

We show that the position-momentum duality offers a transparent interpretation of the band geometry at the topological band crossings. Under this duality, the band geometry with Berry connection is dual to the free-electron motion under gauge field. This identifies the trace of quantum metric as the dual energy in momentum space. The band crossings with Berry defects thus induce the dual energy quantization in the trace of quantum metric. For a \mathbb{Z} nodal-point or nodal-surface semimetal, a dual Landau level quantization occurs owing to the Berry charge. Meanwhile, a nodal-loop semimetal exhibits a Berry vortex line, leading to the quantized dual rotational energy about the nodal loop. A \mathbb{Z}_2 monopole brings about another dual rotational energy, which originates from the link with an additional nodal line. Nontrivial band geometry generically induces finite spread in the Wannier functions. While the spread manifests a quantized lower bound in a \mathbb{Z} nodal-point or nodal-surface semimetal, logarithmic divergence occurs in a nodal-loop semimetal. The band geometry at the band crossings may be probed experimentally by a periodic-drive measurement.

The modern study of gapless topological systems have uncovered various unconventional band crossings with fascinating phenomena. A band crossing in three dimensions (3D) may occur at a nodal point [1–11], a nodal line [1, 12–18], or a nodal surface [15, 17, 19, 20] (Fig. 1). These band crossings are realized in the semimetallic phases of solid-state materials [1], the topological superconductors [21–26], and the spin liquids [27]. Recent studies of synthetic quantum matter present another set of platforms for the band crossings, including the ultracold atomic systems [28, 29], the photonic systems [30], and the superconducting circuits [31, 32]. Distinct band-topology classifications are defined based on the symmetries and the band-crossing structures [33]. For the 3D gapless topological systems, the topological classifications involve the \mathbb{Z} and \mathbb{Z}_2 classifications. Various types of integer topological invariants are proposed as the indicators of these classifications. For example, a \mathbb{Z} nodal point [Fig. 1(a)] carries a Berry monopole, leading to a quantized Chern number under an enclosing-surface integration [34]. The inflation of a \mathbb{Z} nodal point may realize a \mathbb{Z} nodal surface [Fig. 1(b)] [23, 24], where the Berry-charge scenario still apply [19]. A nodal line in a combined parity and time-reversal PT symmetric system can carry a \mathbb{Z}_2 monopole [14, 16]. The according topological invariant corresponds to the linking number with additional nodal lines [Fig. 1(d)] [18].

The band crossings also bring about nontrivial quantum geometry of the bands [35]. The band geometry is characterized by the quantum metric, which measures the state variation under momentum change [36–38]. The components of quantum metric may be probed experimentally, for example, by a periodic drive [39, 40]. Recent studies have uncovered various manifestations of the quantum metric. The integrated trace of quantum metric defines a lower bound of the spread of Wannier functions [41–44], which can be measured directly in the

experiments [39, 45–50]. The finite spread can trigger anomalous superfluid stiffness on flat bands, leading to the geometric enhancement of flat-band superconductivity [35, 51–55]. It can also lead to finite current noise even in the insulating phase [56]. Other works have adopted the quantum metric as an indicator of phase transitions [57–59], fractional Chern insulators [60–62], excitons [63], and orbital susceptibilities [64, 65].

While the bulk of the literature focuses on the extrinsic manifestations of the quantum metric, its intrinsic character has not received sufficient investigation. This direction is recently explored in the context of nodal-point semimetals. The trace of quantum metric receives a transparent interpretation in the chiral multifold semimetals [35]. Under the position-momentum duality, the trace of quantum metric is dual to the kinetic energy on the Haldane sphere [66], thereby acquiring a dual Landau level quantization from the Berry monopole. On the other hand, the integrated determinant of quantum metric over an enclosing surface is proposed as a measure of the Berry defect [67, 68]. These results exemplify the nature of the quantum metric at the nodal points. A natural question then arises as whether these scenarios are applicable to the other topological systems.

In this Letter, we show that the position-momentum duality [35] offers a unified framework of the band geometry at the topological band crossings. Under this duality, the band geometry with Berry connection is dual to the free-electron motion under gauge field. This identifies the trace of quantum metric as the dual energy in momentum space. The band crossings with Berry defects thus induce the dual energy quantization in the trace of quantum metric. For a \mathbb{Z} nodal-point or nodal-surface semimetal, a dual Landau level quantization occurs owing to the Berry charge. Meanwhile, a nodal-loop semimetal exhibits a Berry vortex line, leading to the quantized dual rotational energy about the nodal loop.

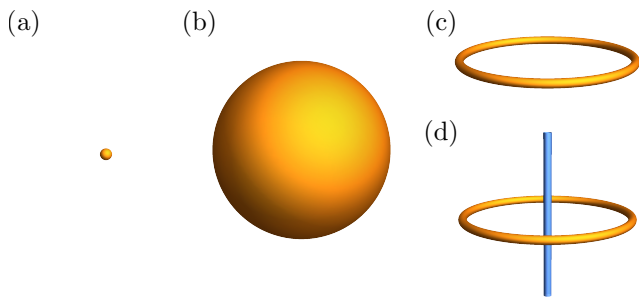


FIG. 1. Band crossings in the 3D Brillouin zone. (a) Nodal point. (b) Nodal surface. (c) \mathbb{Z}_2 -trivial nodal loop. (d) \mathbb{Z}_2 -nontrivial nodal loop.

A \mathbb{Z}_2 monopole brings about another dual rotational energy, which originates from the link with an additional nodal line. The spread of Wannier functions manifests a quantized lower bound in a \mathbb{Z} nodal-point or nodal-surface semimetal, while logarithmic divergence occurs in a nodal-loop semimetal. Our duality-based analysis paves the way for advanced comprehension of nontrivial band geometry at the topological band crossings.

We begin with an introduction to the band geometry. Consider a band with the Bloch eigenstate $|u_{\mathbf{k}}\rangle$, which generically evolves under the variation of momentum \mathbf{k} . Such an evolution manifests the variations in the phase and the state. A quantitative measure is provided by the quantum geometric tensor [69]

$$T_{ab\mathbf{k}} = \langle \partial_{k_a} u_{\mathbf{k}} | (1 - |u_{\mathbf{k}}\rangle\langle u_{\mathbf{k}}|) | \partial_{k_b} u_{\mathbf{k}} \rangle \quad (1)$$

with $a, b = x, y, z$. The real part $g_{ab\mathbf{k}} = \text{Re}[T_{ab\mathbf{k}}]$ is the quantum or Fubini-Study metric [36–38], which captures the quantum distance under state variation $1 - |\langle u_{\mathbf{k}} | u_{\mathbf{k}+d\mathbf{k}} \rangle|^2 = g_{ab\mathbf{k}} dk_a dk_b$. On the other hand, the imaginary part measures the phase variation and the according Berry flux $B_{a\mathbf{k}} = -\epsilon_{abc} \text{Im}[T_{bc\mathbf{k}}]$ [34, 70]. Define the Berry connection $\mathbf{A}_{\mathbf{k}} = \langle u_{\mathbf{k}} | i\nabla_{\mathbf{k}} | u_{\mathbf{k}} \rangle$ as a momentum-space gauge field under nontrivial band geometry [34]. The quantum metric and the Berry flux become [71]

$$g_{ab\mathbf{k}} = \frac{1}{2} \langle u_{\mathbf{k}} | \{r_a, r_b\} | u_{\mathbf{k}} \rangle, \quad \mathbf{B}_{\mathbf{k}} = \nabla_{\mathbf{k}} \times \mathbf{A}_{\mathbf{k}}, \quad (2)$$

where the position $\mathbf{r} = i\nabla_{\mathbf{k}} - \mathbf{A}_{\mathbf{k}}$ is a momentum-space covariant derivative. The effect of Berry flux as a momentum-space “magnetic field” has been studied extensively [34]. Here we focus on the quantum metric and search for useful indications to the band geometry.

The individual components of quantum metric are usually complicated and hard to interpret. Nevertheless, the trace of quantum metric takes a profound form [35]

$$\text{Tr}g_{\mathbf{k}} = \langle |\mathbf{r}|^2 \rangle, \quad (3)$$

where the expectation value $\langle \dots \rangle = \langle u_{\mathbf{k}} | \dots | u_{\mathbf{k}} \rangle$ of momentum-space Laplacian $|\mathbf{r}|^2$ is measured. Significantly, this quantity captures the “dual energy” of a free

particle in momentum space, which carries a half-unity “dual mass” and experiences the Berry connection. We thus establish a position-momentum duality between the band geometry and the free-particle motion under gauge field. The duality presents a feasible solution to the interpretation of the band geometry. If the duality leads to a simple free-particle model with well-studied solution, the trace of quantum metric can be understood under a direct inference. Similar concept of position-momentum duality was proposed previously in the context of harmonic traps [72–74] and fractional Chern insulators [61, 62]. These works adopted the confinement potential $V(\mathbf{r}) \sim |\mathbf{r}|^2$ to insert the band-geometry contribution into the actual electronic energy. In comparison, our analysis directly identifies the trace of quantum metric as the true dual energy in momentum space. This deepens the comprehension of the band geometry as the dual free-particle theory of general bands.

We now introduce how the duality operates on the nontrivial band geometry. Here we focus on the 3D gapless topological systems, where approximate rotation symmetries can occur near the band crossings. Under such symmetries, simple models become available to the dual free-particle theories. A band crossing can host a defect of Berry connection and induce nontrivial band geometry. We will show that this feature is encoded in the “dual energy quantization” in the trace of quantum metric. This scenario is applicable to both \mathbb{Z} and \mathbb{Z}_2 gapless topological systems.

We first study the \mathbb{Z} gapless topological systems with the duality. As a paradigmatic example, we present the analysis of the chiral multifold semimetals (CMS) [35], which constitute a large family of \mathbb{Z} nodal-point semimetals. The band crossings in these systems occur at distinct points [Fig. 1(a)] [1–4, 75]. At each nodal point, the low-energy theory manifests the chiral fermions with multifold degeneracy [Fig. 2(a)]. A minimal model exhibits a rotationally symmetric spin- s Hamiltonian with integer or half-integer spin $s = 1/2, 1, 3/2, \dots$

$$\mathcal{H}_{\text{CMS},\mathbf{k}} = v\mathbf{k} \cdot \mathbf{S}. \quad (4)$$

Here v is the effective velocity, $\mathbf{k} = k\hat{\mathbf{k}}$ with magnitude k and direction $\hat{\mathbf{k}}$, and $\mathbf{S} = (S^x, S^y, S^z)$ is the spin- s representation. There are $2s + 1$ bands in this model, carrying the dispersion energies $\varepsilon_{\mathbf{k}}^{sn} = vkn$ with $n = -s, -s + 1, \dots, s$. In accordance with the Berry flux $\mathbf{B}_{\mathbf{k}}^{sn} = -(n/k^2)\hat{\mathbf{k}}$, the nodal point at $\mathbf{k} = \mathbf{0}$ carries a quantized Berry monopole $q^{sn} = -n$. This monopole charge corresponds to the Chern number $C^{sn} = (1/2\pi) \oint d\mathbf{S}_{\mathbf{k}} \cdot \mathbf{B}_{\mathbf{k}}^{sn} = 2q^{sn} = -2n$ under an enclosing-surface integration, which is the topological invariant. The rotationally symmetric structure around the monopole indicates the duality to a Haldane sphere [66, 76, 77]. Analogous to the quantum Hall effect on the Haldane sphere, the “dual Landau level quantization”

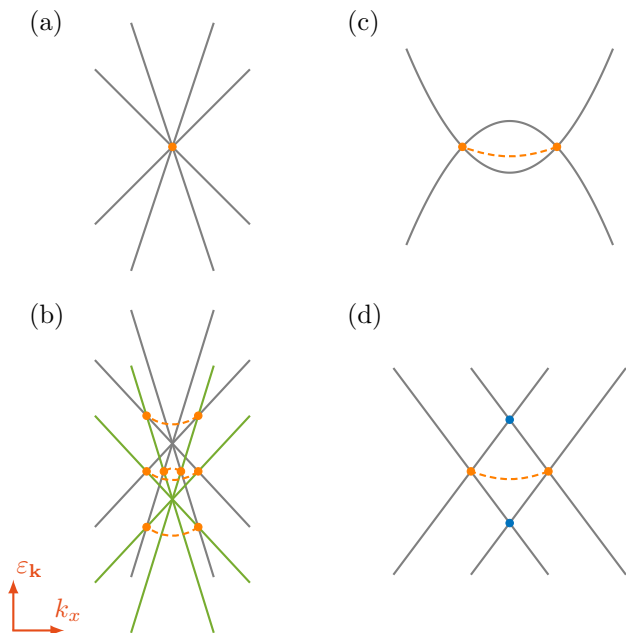


FIG. 2. The band structures in the minimal models for the (a) nodal-point, (b) nodal-surface, (c) \mathbb{Z}_2 -trivial nodal-loop, and (d) \mathbb{Z}_2 -nontrivial nodal-loop semimetals. The band crossings are indicated by the same colors as in Fig. 1. The points belonging to the same band crossing are connected by a dashed curve.

occurs in the trace of quantum metric herein [35]. An alternative form of the Hamiltonian $\tilde{\mathcal{H}}_{\text{CMS},\mathbf{k}} = vk\hat{\mathbf{k}} \cdot \mathbf{S}$ indicates that the wave functions are independent of k . Due to the absence of radial contribution, the trace of quantum metric $\text{Tr}g_{\text{CMS},\mathbf{k}}^{sn} = \langle |\mathbf{\Lambda}^{sn}|^2/k^2 \rangle$ measures the dual rotational energy of the dynamical angular momentum $\mathbf{\Lambda}^{sn} = \mathbf{r}^{sn} \times \mathbf{k}$. Note that the angular momentum under rotation symmetry takes the form $\mathbf{L}^{sn} = \mathbf{\Lambda}^{sn} + q^{sn}\hat{\mathbf{k}}$. With $|\mathbf{\Lambda}^{sn}|^2 = |\mathbf{L}^{sn}|^2 - (q^{sn})^2$, we obtain the quantized trace of quantum metric

$$\text{Tr}g_{\text{CMS},\mathbf{k}}^{sn} = \frac{1}{k^2}[s(s+1) - (q^{sn})^2], \quad (5)$$

labeled by the angular momentum s and the monopole charge q^{sn} . This exemplifies the quantized band geometry from the dual Haldane sphere in the \mathbb{Z} nodal-point semimetals.

The duality can also be adopted to the \mathbb{Z} nodal-surface (NS) semimetals [19], which accommodate two-band crossings on closed surfaces [Fig. 1(b)]. The \mathbb{Z} nodal surface may be realized, for example, from a pair of degenerate chiral multifold semimetallic points \mathbf{P}_{\pm} . When the degeneracy is broken by an energy splitting $\Delta\varepsilon_0 = \varepsilon_0^+ - \varepsilon_0^- > 0$ [Fig. 2(b)], the bands from different nodal points cross at spherical nodal surfaces. As inflated nodal points [23], these nodal surfaces inherit the \mathbb{Z} topological structures of the original nodal points. Consider the low-energy theory of a nodal surface below charge

neutrality, which is formed by the n_+ -th and n_- -th original bands. For the lower band, the band eigenstate corresponds to the n_{\mp} -th original band inside(outside) the nodal surface. This implies the occurrence of different Berry fluxes $\mathbf{B}_{\mathbf{k}}^{\text{in/out}} = \mathbf{B}_{\mathbf{k}}^{sn_{\mp}}$ and according Chern numbers $C^{\text{in/out}} = C^{sn_{\mp}}$ in the two regions. A topological invariant is defined by the change of Chern number across the nodal surface $\Delta C = C^{\text{in}} - C^{\text{out}}$ [19]. The quantum metric can also be inferred directly, with the individual components in the spin-1/2 case derived in Ref. 78. We present an interpretation based on the duality. The low-energy theory is dual to a free-particle model with a “uniformly-charged magnetic spherical shell” and a magnetic monopole at the origin. While the monopole charge is $q = C^{\text{in}}/2$, the spherical shell carries the total charge $Q = \Delta C/2$ corresponding to the topological invariant. The Berry charges induce the dual Landau level quantization in the trace of quantum metric

$$\text{Tr}g_{\text{NS},\mathbf{k}}^{\text{in/out}} = \text{Tr}g_{\text{CMS},\mathbf{k}}^{sn_{\mp}}. \quad (6)$$

Analogous results hold for the upper band. Notably, the band geometry exhibit different structures on different sides of the nodal surface. This feature is attributed to the Berry charge at the nodal surface and is generic in the \mathbb{Z} nodal-surface semimetals.

We next turn to the analysis of \mathbb{Z}_2 gapless topological systems. Before diving into the 3D systems, we discuss how the dual energy quantization occurs at the two-dimensional (2D) Dirac point (2DDP). This example will serve as an important hint to the 3D \mathbb{Z}_2 gapless topological systems. A minimal model at the 2D Dirac point takes a rotationally symmetric form [79]

$$\mathcal{H}_{2\text{DDP},\mathbf{k}}^l = v(k_+^{2l}\sigma^- + k_-^{2l}\sigma^+) \quad (7)$$

with $k_{\pm} = k_x \pm ik_y$, $l = 1/2, 1, 3/2, \dots$, and Pauli matrices $\sigma^{\pm} = (\sigma^x \pm i\sigma^y)/2$. This system contains two bands with dispersion energies $\varepsilon_{\mathbf{k}}^{\pm} = \pm vk^{2l}$, which become degenerate at the Dirac point $\mathbf{k} = \mathbf{0}$. The Berry connection forms a vortex structure around the Dirac point, thereby driving a $2\pi l$ phase winding in the band eigenstates. Accordingly, the Berry flux experiences a singularity at the Dirac point and vanishes everywhere else. The trace of quantum metric is determined by this Berry vortex structure. According to the Hamiltonian $\mathcal{H}_{2\text{DDP},\mathbf{k}}^l = vk^{2l}(\hat{k}_+^{2l}\sigma^- + \hat{k}_-^{2l}\sigma^+)$, the wave functions are k -independent. Without the radial contribution, the trace of quantum metric measures the dual rotational energy $\text{Tr}g_{2\text{DDP},\mathbf{k}}^{ln} = \langle (\Lambda_z^{ln})^2/k^2 \rangle$. Here $\Lambda_z^{ln} = L_z^{ln}$ serves as the angular momentum since the Berry monopole is absent. The magnitude $|L_z^{ln}| = l$ corresponds to the $2\pi l$ phase winding around the Dirac point. We arrive at the dual energy quantization in the trace of quantum metric

$$\text{Tr}g_{2\text{DDP},\mathbf{k}}^{ln} = \frac{l^2}{k^2}, \quad (8)$$

consistent with a direct calculation for graphene when $l = 1/2$ [52]. Our analysis indicates how the duality works on the band geometry from Berry vortices.

The result at the 2D Dirac point can be generalized to the 3D \mathbb{Z}_2 gapless topological systems. A natural generalization occurs in the nodal-loop semimetals, where the band crossings take place along closed loops [Fig. 1(c)] [12–18]. Consider a minimal two-band model of the nodal-loop semimetals [22, 80]

$$\mathcal{H}_{\text{NL},\mathbf{k}}(\Delta) = \frac{k_{\perp}^2 - \Delta}{2m} \sigma^x + v_z k_z \sigma^y, \quad (9)$$

where $k_{\perp} = (k_x^2 + k_y^2)^{1/2}$ and $\Delta > 0$. This system shows a nodal loop in the k_x - k_y plane at charge neutrality [Fig. 2(c)], which is defined by the major radius $k_R = \sqrt{\Delta}$. Assume an isotropic dispersion around the nodal loop $v_{\perp} = k_R/m = v_z = v$. A linearization at low energy leads to the $l = 1/2$ case of the general minimal model [81, 82]

$$\mathcal{H}_{\text{NL},\mathbf{k}}^l = v(k_{r,+}^{2l} \sigma^- + k_{r,-}^{2l} \sigma^+), \quad (10)$$

where $k_{r,\pm} = (k_{\perp} - k_R) \pm i k_z$ are defined around the nodal loop. This model obeys two rotation symmetries, which are about the nodal loop and the $k_{\perp} = 0$ line at loop center, respectively. The two bands exhibit the dispersion energies $\varepsilon_{\mathbf{k}}^{\pm} = \pm v k_r^{2l}$, where $k_r = [(k_{\perp} - k_R)^2 + k_z^2]^{1/2}$ is the minor radius from the nodal loop. Importantly, the model serves as a “stacking” of the 2D Dirac-point systems along the nodal loop. This identifies the nodal loop as a Berry vortex line, a generalization from the Berry vortex at the 2D Dirac point. The $2\pi l$ phase winding now occurs around the nodal loop. Accordingly, the Berry flux experiences a singularity along the nodal loop and vanishes everywhere else. The Berry vortex line induces the dual rotational energy of the axial angular momentum $|L_{\hat{\phi}}^{ln}| = l$, where $\hat{\phi}$ is the tangent unit vector along the nodal loop. The trace of quantum metric thus exhibits the dual energy quantization

$$\text{Tr} g_{\text{NL},\mathbf{k}}^{ln} = \frac{l^2}{k_r^2}, \quad (11)$$

similar to the result at the 2D Dirac point. Note that the nodal loop in $\mathcal{H}_{\text{NL},\mathbf{k}}(\Delta)$ shrinks to a point and vanishes when Δ decreases and turns negative. Since the nodal loop can be annihilated by itself, it is \mathbb{Z}_2 -trivial in the topological classification [14].

There also exist nodal loops which are \mathbb{Z}_2 -nontrivial [14, 16–18]. These nodal loops are realized under combined parity and time-reversal PT -symmetry, which imposes the reality condition on the systems. Consider a minimal model of the \mathbb{Z}_2 -nontrivial nodal loops [14]

$$\mathcal{H}_{\mathbb{Z}_2\text{NL},\mathbf{k}} = v k_x \sigma^x + v k_y \tau^y \sigma^y + v k_z \sigma^z + m \tau^x \sigma^x, \quad (12)$$

where the Pauli matrices σ^a and τ^a are defined. This model accommodates four bands with the dispersion energies $\varepsilon_{\mathbf{k}}^{\pm\pm} = \pm v [(k_{\perp} \pm k_R)^2 + k_z^2]^{1/2}$ for $k_R = |m|/v$. At

finite $|m| > 0$, the two middle bands form a nodal loop at charge neutrality with major radius k_R [Fig. 2(d)]. These two bands obey the same rotation symmetries as the model of \mathbb{Z}_2 -trivial nodal loops. Similar to the \mathbb{Z}_2 -trivial nodal loop with $l = 1/2$, the nodal loop herein serves as a Berry vortex line for a π phase winding. An important difference is the interplay with an additional nodal line $k_{\perp} = 0$ at finite energy [18]. For the upper(lower) band, the additional nodal line occurs at the band crossing with the highest(lowest) band. This additional nodal line penetrates the center of the nodal loop, leading to a topologically nontrivial “link” [Fig. 1(d)]. The link with the nodal line defines a \mathbb{Z}_2 monopole at the nodal loop. This monopole drives the nodal loop \mathbb{Z}_2 -nontrivial, which shrinks to a point (when $m = 0$) at most under changing m . The \mathbb{Z}_2 -nontrivial nodal loops can only be annihilated through the pair annihilation.

The link of the \mathbb{Z}_2 monopole is encoded in the band geometry. We calculate the quantum metric for the two middle bands in the minimal model. The individual components of quantum metric are complicated, with the special cases derived at $k_z = 0$ in Ref. 78. Nevertheless, the trace of quantum metric is amiable according to the duality. It can be shown that the wave functions are independent of the radial components k_r and k_R . This indicates the absence of radial contributions in the trace of quantum metric, leaving only the angular contributions. We further uncover that each wave function is a tensor product of two \mathbb{Z}_2 -trivial wave functions, which are at the nodal loop and the additional nodal line, respectively. A direct calculation obtains the according dual rotational energy in the trace of quantum metric

$$\text{Tr} g_{\mathbb{Z}_2\text{NL},\mathbf{k}} = \frac{1}{4k_r^2} + \frac{1}{4k_{\perp}^2}. \quad (13)$$

The first term is the dual rotational energy about the nodal loop, which is identical to the \mathbb{Z}_2 -trivial case with $l = 1/2$. Meanwhile, the second term captures the dual rotational energy of the axial angular momentum $|L_z^2| = 1/2$ about the additional nodal line. The presence of this term clearly indicates the link of the \mathbb{Z}_2 monopole, which is absent for the \mathbb{Z}_2 -trivial nodal loop. We thus arrive at a clear interpretation of the nontrivial band geometry in the \mathbb{Z}_2 nodal-loop semimetals.

A direct manifestation of the band geometry occurs in the spread of Wannier functions [35, 41–44, 83]. For the Wannier functions of a band, the spread functional $\Omega = \langle \mathbf{r}^2 \rangle - \langle \mathbf{r} \rangle^2$ exhibits the gauge-invariant lower bound $\Omega_{\text{GI}} = \mathcal{V}_0 \Sigma$ with $\Sigma = \int_{\mathbf{k}} \text{Tr} g_{\mathbf{k}}$. Here \mathcal{V}_0 is the unit-cell volume and $\int_{\mathbf{k}} = \int d^3k / (2\pi)^3$. As the integrated trace of quantum metric, the gauge-invariant lower bound originates solely from the band geometry. An estimation $\Sigma_{\text{SR}} = \int_{\text{SR},\mathbf{k}} \text{Tr} g_{\mathbf{k}} \leq \Sigma$ can be further obtained by the focus on a subregion (SR). We consider this estimation in the 3D gapless topological systems, where the strongest contributions usually arise near the band cross-

ings. For the chiral multifold semimetals, the estimated lower bound $\Sigma_{\text{CMF}}^{sn} = (\Lambda_k/4\pi^2)G^{sn}$ is quantized [35]. Here $G^{sn} = (1/2\pi) \oint d\mathbf{S}_k \cdot \hat{\mathbf{k}} \text{Tr} g_{\text{CMS},k}^{sn} = 2[s(s+1) - (q^{sn})^2]$ is a quantized enclosing-surface integration, and Λ_k is an ultraviolet (UV) cutoff of k . The quantized result also applies to the \mathbb{Z} nodal-surface semimetals. Meanwhile, the nodal-loop semimetals exhibit significantly different features. For the \mathbb{Z}_2 -trivial nodal loop, the estimated lower bound is logarithmically divergent $\Sigma_{\text{NL}}^{ln} = (1/4\pi^2)(2\pi k_R)l^2 \log k_r|_0^{\Lambda_{k_r}}$, where Λ_{k_r} defines the UV cutoff of k_r . This result is a direct generalization from the logarithmic divergence at the 2D Dirac point. The \mathbb{Z}_2 -nontrivial nodal loop exhibits an additional logarithmic divergence $\sim \ln k_{\perp}|_0$ due to the link of the \mathbb{Z}_2 monopole. This distinguishes the estimated lower bound of the \mathbb{Z}_2 -nontrivial nodal loop from the \mathbb{Z}_2 -trivial one. Due to the logarithmic divergences, the band geometry may have stronger manifestations at the nodal loops than at the other band crossings.

The gauge-invariant lower bound can be probed directly with a periodic drive [39]. Under a linear shake along a direction $\hat{\mathbf{a}}$, the integrated quantum metric $\int_{\mathbf{k}} g_{aa\mathbf{k}}$ of the occupied bands corresponds to the excitation rate. The integrated trace of quantum metric is then obtained from the measurements along all three directions $a = x, y, z$, which determines the gauge-invariant lower bound. Such a measurement has been performed experimentally in an ultracold atomic Floquet Chern insulator [46]. Most of the current measurements apply to the integrated trace of quantum metric in all occupied bands. The probe with momentum and band resolutions will advance the understanding of band geometry in the gapless topological systems [39, 40, 84].

In summary, we show that the position-momentum duality offers a transparent interpretation of the band geometry at the topological band crossings. The trace of quantum metric provides a unified framework through this duality, which is achieved by encoding the dual rotational energy about the band crossings with nontrivial Berry defects. This scenario applies to the \mathbb{Z} nodal-point and nodal-surface semimetals, as well as the \mathbb{Z}_2 nodal-loop semimetals. The simple quantization rules may be broken by the symmetry-breaking perturbations, such as those far away from the band crossings. Nevertheless, the results in our analysis, such as the integrated trace of quantum metric, may remain close to the quantized values until the band crossing structures completely vanish. Our duality-based analysis offers a feasible route toward further understanding of nontrivial band geometry. The investigations in the other gapless topological systems, such as the gapless topological superconductors [21–26] and spin liquids [27], degenerate bands with non-Abelian Berry connections [58], or higher-dimensional systems with tensor monopoles [40, 67], may serve as interesting topics for future work.

The authors thank Nathan Goldman, Ching Hua Lee, and especially Rahul Nandkishore for fruitful discussions and feedback on the manuscript. YPL was sponsored by the Army Research Office under Grant No. W911NF-17-1-0482. The views and conclusions contained in this document are those of the authors and should not be interpreted as representing the official policies, either expressed or implied, of the Army Research Office or the U.S. Government. The U.S. Government is authorized to reproduce and distribute reprints for Government purposes notwithstanding any copyright notation herein. YPL also acknowledges Ying-Jer Kao for the hospitality at National Taiwan University during the pandemic.

-
- [1] N. P. Armitage, E. J. Mele, and A. Vishwanath, *Rev. Mod. Phys.* **90**, 015001 (2018).
 - [2] B. Bradlyn, J. Cano, Z. Wang, M. G. Vergniory, C. Felser, R. J. Cava, and B. A. Bernevig, *Science* **353**, aaf5037 (2016).
 - [3] H. Isobe and L. Fu, *Phys. Rev. B* **93**, 241113 (2016).
 - [4] P. Tang, Q. Zhou, and S.-C. Zhang, *Phys. Rev. Lett.* **119**, 206402 (2017).
 - [5] I. Boettcher, *Phys. Rev. Lett.* **124**, 127602 (2020).
 - [6] Z. Rao, H. Li, T. Zhang, S. Tian, C. Li, B. Fu, C. Tang, L. Wang, Z. Li, W. Fan, J. Li, Y. Huang, Z. Liu, Y. Long, C. Fang, H. Weng, Y. Shi, H. Lei, Y. Sun, T. Qian, and H. Ding, *Nature* **567**, 496 (2019).
 - [7] D. S. Sanchez, I. Belopolski, T. A. Cochran, X. Xu, J.-X. Yin, G. Chang, W. Xie, K. Manna, V. Süß, C.-Y. Huang, N. Alidoust, D. Multer, S. S. Zhang, N. Shumiya, X. Wang, G.-Q. Wang, T.-R. Chang, C. Felser, S.-Y. Xu, S. Jia, H. Lin, and M. Z. Hasan, *Nature* **567**, 500 (2019).
 - [8] N. B. M. Schröter, D. Pei, M. G. Vergniory, Y. Sun, K. Manna, F. de Juan, J. A. Krieger, V. Süss, M. Schmidt, P. Dudin, B. Bradlyn, T. K. Kim, T. Schmitt, C. Cacho, C. Felser, V. N. Strocov, and Y. Chen, *Nat. Phys.* **15**, 759 (2019).
 - [9] D. Takane, Z. Wang, S. Souma, K. Nakayama, T. Nakamura, H. Oinuma, Y. Nakata, H. Iwasawa, C. Cacho, T. Kim, K. Horiba, H. Kumigashira, T. Takahashi, Y. Ando, and T. Sato, *Phys. Rev. Lett.* **122**, 076402 (2019).
 - [10] B. Q. Lv, Z.-L. Feng, J.-Z. Zhao, N. F. Q. Yuan, A. Zong, K. F. Luo, R. Yu, Y.-B. Huang, V. N. Strocov, A. Chikina, A. A. Soluyanov, N. Gedik, Y.-G. Shi, T. Qian, and H. Ding, *Phys. Rev. B* **99**, 241104 (2019).
 - [11] N. B. M. Schröter, S. Stolz, K. Manna, F. de Juan, M. G. Vergniory, J. A. Krieger, D. Pei, T. Schmitt, P. Dudin, T. K. Kim, C. Cacho, B. Bradlyn, H. Borrmann, M. Schmidt, R. Widmer, V. N. Strocov, and C. Felser, *Science* **369**, 179 (2020).
 - [12] J.-M. Carter, V. V. Shankar, M. A. Zeb, and H.-Y. Kee, *Phys. Rev. B* **85**, 115105 (2012).
 - [13] H. Weng, C. Fang, Z. Fang, B. A. Bernevig, and X. Dai, *Phys. Rev. X* **5**, 011029 (2015).
 - [14] C. Fang, Y. Chen, H.-Y. Kee, and L. Fu, *Phys. Rev. B* **92**, 081201 (2015).

- [15] Q.-F. Liang, J. Zhou, R. Yu, Z. Wang, and H. Weng, *Phys. Rev. B* **93**, 085427 (2016).
- [16] Y. X. Zhao and Y. Lu, *Phys. Rev. Lett.* **118**, 056401 (2017).
- [17] T. Bzdušek and M. Sigrist, *Phys. Rev. B* **96**, 155105 (2017).
- [18] J. Ahn, D. Kim, Y. Kim, and B.-J. Yang, *Phys. Rev. Lett.* **121**, 106403 (2018).
- [19] O. Türker and S. Moroz, *Phys. Rev. B* **97**, 075120 (2018).
- [20] W. Wu, Y. Liu, S. Li, C. Zhong, Z.-M. Yu, X.-L. Sheng, Y. X. Zhao, and S. A. Yang, *Phys. Rev. B* **97**, 115125 (2018).
- [21] M. Sigrist and K. Ueda, *Rev. Mod. Phys.* **63**, 239 (1991).
- [22] R. Nandkishore, *Phys. Rev. B* **93**, 020506 (2016).
- [23] D. F. Agterberg, P. M. R. Brydon, and C. Timm, *Phys. Rev. Lett.* **118**, 127001 (2017).
- [24] P. M. R. Brydon, D. F. Agterberg, H. Menke, and C. Timm, *Phys. Rev. B* **98**, 224509 (2018).
- [25] J. W. F. Venderbos, L. Savary, J. Ruhman, P. A. Lee, and L. Fu, *Phys. Rev. X* **8**, 011029 (2018).
- [26] J. M. Link and I. F. Herbut, *Phys. Rev. Lett.* **125**, 237004 (2020).
- [27] L. Savary and L. Balents, *Rep. Prog. Phys.* **80**, 016502 (2016).
- [28] N. R. Cooper, J. Dalibard, and I. B. Spielman, *Rev. Mod. Phys.* **91**, 015005 (2019).
- [29] B. Song, C. He, S. Niu, L. Zhang, Z. Ren, X.-J. Liu, and G.-B. Jo, *Nat. Phys.* **15**, 911 (2019).
- [30] T. Ozawa, H. M. Price, A. Amo, N. Goldman, M. Hafezi, L. Lu, M. C. Rechtsman, D. Schuster, J. Simon, O. Zeitler, and I. Carusotto, *Rev. Mod. Phys.* **91**, 015006 (2019).
- [31] X. Tan, D.-W. Zhang, Q. Liu, G. Xue, H.-F. Yu, Y.-Q. Zhu, H. Yan, S.-L. Zhu, and Y. Yu, *Phys. Rev. Lett.* **120**, 130503 (2018).
- [32] X. Tan, Y. X. Zhao, Q. Liu, G. Xue, H.-F. Yu, Z. D. Wang, and Y. Yu, *Phys. Rev. Lett.* **122**, 010501 (2019).
- [33] C.-K. Chiu, J. C. Y. Teo, A. P. Schnyder, and S. Ryu, *Rev. Mod. Phys.* **88**, 035005 (2016).
- [34] D. Xiao, M.-C. Chang, and Q. Niu, *Rev. Mod. Phys.* **82**, 1959 (2010).
- [35] Y.-P. Lin and W.-H. Hsiao, *Phys. Rev. B* **103**, L081103 (2021).
- [36] J. P. Provost and G. Vallee, *Commun. Math. Phys.* **76**, 289 (1980).
- [37] D. N. Page, *Phys. Rev. A* **36**, 3479 (1987).
- [38] J. Anandan and Y. Aharonov, *Phys. Rev. Lett.* **65**, 1697 (1990).
- [39] T. Ozawa and N. Goldman, *Phys. Rev. B* **97**, 201117 (2018).
- [40] M. Chen, C. Li, G. Palumbo, Y.-Q. Zhu, N. Goldman, and P. Cappellaro, arXiv e-prints, arXiv:2008.00596 (2020), arXiv:2008.00596 [quant-ph].
- [41] N. Marzari and D. Vanderbilt, *Phys. Rev. B* **56**, 12847 (1997).
- [42] S. Matsuura and S. Ryu, *Phys. Rev. B* **82**, 245113 (2010).
- [43] N. Marzari, A. A. Mostofi, J. R. Yates, I. Souza, and D. Vanderbilt, *Rev. Mod. Phys.* **84**, 1419 (2012).
- [44] C. H. Lee and X.-L. Qi, *Phys. Rev. B* **90**, 085103 (2014).
- [45] O. Bleu, D. D. Solnyshkov, and G. Malpuech, *Phys. Rev. B* **97**, 195422 (2018).
- [46] L. Asteria, D. T. Tran, T. Ozawa, M. Tarnowski, B. S. Rem, N. Fläschner, K. Sengstock, N. Goldman, and C. Weitenberg, *Nat. Phys.* **15**, 449 (2019).
- [47] R. L. Klees, G. Rastelli, J. C. Cuevas, and W. Belzig, *Phys. Rev. Lett.* **124**, 197002 (2020).
- [48] M. Yu, P. Yang, M. Gong, Q. Cao, Q. Lu, H. Liu, S. Zhang, M. B. Plenio, F. Jelezko, T. Ozawa, N. Goldman, and J. Cai, *Nat. Sci. Rev.* **7**, 254 (2019).
- [49] X. Tan, D.-W. Zhang, Z. Yang, J. Chu, Y.-Q. Zhu, D. Li, X. Yang, S. Song, Z. Han, Z. Li, Y. Dong, H.-F. Yu, H. Yan, S.-L. Zhu, and Y. Yu, *Phys. Rev. Lett.* **122**, 210401 (2019).
- [50] A. Gianfrate, O. Bleu, L. Dominici, V. Ardizzone, M. De Giorgi, D. Ballarini, G. Lerario, K. W. West, L. N. Pfeiffer, D. D. Solnyshkov, D. Sanvitto, and G. Malpuech, *Nature* **578**, 381 (2020).
- [51] S. Peotta and P. Törmä, *Nat. Commun.* **6**, 8944 (2015).
- [52] L. Liang, T. I. Vanhala, S. Peotta, T. Siro, A. Harju, and P. Törmä, *Phys. Rev. B* **95**, 024515 (2017).
- [53] X. Hu, T. Hyart, D. I. Pikulin, and E. Rossi, *Phys. Rev. Lett.* **123**, 237002 (2019).
- [54] F. Xie, Z. Song, B. Lian, and B. A. Bernevig, *Phys. Rev. Lett.* **124**, 167002 (2020).
- [55] Y.-P. Lin, *Phys. Rev. Research* **2**, 043209 (2020).
- [56] T. Neupert, C. Chamon, and C. Mudry, *Phys. Rev. B* **87**, 245103 (2013).
- [57] P. Zanardi, P. Giorda, and M. Cozzini, *Phys. Rev. Lett.* **99**, 100603 (2007).
- [58] Y.-Q. Ma, S. Chen, H. Fan, and W.-M. Liu, *Phys. Rev. B* **81**, 245129 (2010).
- [59] M. Kolodrubetz, V. Gritsev, and A. Polkovnikov, *Phys. Rev. B* **88**, 064304 (2013).
- [60] R. Roy, *Phys. Rev. B* **90**, 165139 (2014).
- [61] M. Claassen, C. H. Lee, R. Thomale, X.-L. Qi, and T. P. Devereaux, *Phys. Rev. Lett.* **114**, 236802 (2015).
- [62] C. H. Lee, M. Claassen, and R. Thomale, *Phys. Rev. B* **96**, 165150 (2017).
- [63] A. Srivastava and A. Imamoğlu, *Phys. Rev. Lett.* **115**, 166802 (2015).
- [64] Y. Gao, S. A. Yang, and Q. Niu, *Phys. Rev. B* **91**, 214405 (2015).
- [65] F. Piéchon, A. Raoux, J.-N. Fuchs, and G. Montambaux, *Phys. Rev. B* **94**, 134423 (2016).
- [66] F. D. M. Haldane, *Phys. Rev. Lett.* **51**, 605 (1983).
- [67] G. Palumbo and N. Goldman, *Phys. Rev. Lett.* **121**, 170401 (2018).
- [68] Y. Hwang, J. Jung, J.-W. Rhim, and B.-J. Yang, arXiv e-prints, arXiv:2012.15122 (2020), arXiv:2012.15122 [cond-mat.mes-hall].
- [69] M. V. Berry, in *Geometric Phases in Physics*, edited by A. Shapere and F. Wilczek (World Scientific, Singapore, 1989) p. 7.
- [70] M. V. Berry, *Proc. R. Soc. London, Ser. A* **392**, 45 (1984).
- [71] R. Shankar, “Quantum geometry and topology,” in *Topology and Condensed Matter Physics*, edited by S. M. Bhattarjee, M. Mj, and A. Bandyopadhyay (Springer Singapore, Singapore, 2017) pp. 253–279.
- [72] C.-J. Wu, I. Mondragon-Shem, and X.-F. Zhou, *Chin. Phys. Lett.* **28**, 097102 (2011).
- [73] H. M. Price, T. Ozawa, and I. Carusotto, *Phys. Rev. Lett.* **113**, 190403 (2014).
- [74] T. Ozawa, H. M. Price, and I. Carusotto, *Phys. Rev. B* **93**, 195201 (2016).
- [75] Z. Lan, N. Goldman, A. Bermudez, W. Lu, and P. Öhberg, *Phys. Rev. B* **84**, 165115 (2011).
- [76] J. K. Jain, *Composite Fermions* (Cambridge University

- Press, Cambridge, 2007).
- [77] W.-H. Hsiao, *Phys. Rev. B* **101**, 155310 (2020).
 - [78] G. Salerno, N. Goldman, and G. Palumbo, *Phys. Rev. Research* **2**, 013224 (2020).
 - [79] A. H. Castro Neto, F. Guinea, N. M. R. Peres, K. S. Novoselov, and A. K. Geim, *Rev. Mod. Phys.* **81**, 109 (2009).
 - [80] Y. Huh, E.-G. Moon, and Y. B. Kim, *Phys. Rev. B* **93**, 035138 (2016).
 - [81] Z.-M. Yu, W. Wu, X.-L. Sheng, Y. X. Zhao, and S. A. Yang, *Phys. Rev. B* **99**, 121106 (2019).
 - [82] J.-R. Wang, W. Li, and C.-J. Zhang, *Phys. Rev. B* **102**, 085132 (2020).
 - [83] G. Strinati, *Phys. Rev. B* **18**, 4104 (1978).
 - [84] M. Aidelsburger, M. Lohse, C. Schweizer, M. Atala, J. T. Barreiro, S. Nascimbène, N. R. Cooper, I. Bloch, and N. Goldman, *Nat. Phys.* **11**, 162 (2015).